TISSUE ENGINEERING: Part C
Volume 16, Number 5, 2010

DOI: 10.1089/ten.tec.2009.0444

Fabrication and Repair of Cartilage Defects with a Novel Acellular Cartilage Matrix Scaffold

Ziquan Yang, M.D., Ph.D.,[1,2] Yanyun Shi, M.D.,[3] Xiaochun Wei, M.D., Ph.D.,[1] Junren He, M.D.,[1] Shuhua Yang, M.D., Ph.D.,[4] Glenn Dickson, Ph.D.,[2] Jingqun Tang, M.D., Ph.D.,[2] Juanjuan Xiang, M.D., Ph.D.,[2] Chao Song, M.D., Ph.D.,[2] and Gang Li, M.D., Ph.D.[2,5]

The objectives of this study were to develop a three-dimensional acellular cartilage matrix (ACM) and investigate its possibility for use as a scaffold in cartilage tissue engineering. Bovine articular cartilage was decellularized sequentially with trypsin, nuclease solution, hypotonic buffer, and Triton ×100 solution; molded with freeze-drying process; and cross-linked by ultraviolet irradiation. Histological and biochemical analysis showed that the ACM was devoid of cells and still maintained the collagen and glycosaminoglycan components of cartilage. Scanning electronic microscopy and mercury intrusion porosimetry showed that the ACM had a sponge-like structure of high porosity. The ACM scaffold had good biocompatibility with cultured rabbit bone marrow mesenchymal stem cells with no indication of cytotoxicity both in contact and in extraction assays. The cartilage defects repair in rabbit knees with the mesenchymal stem cell–ACM constructs had a significant improvement of histological scores when compared to the control groups at 6 and 12 weeks. In summary, the ACM possessed the characteristics that afford it as a potential scaffold for cartilage tissue engineering.

Introduction

Articular cartilage plays an important role in the function of diarthrodial joints, providing frictionless motion between the joint surfaces and distributing the mechanical stresses.[1] However, because of its avascular nature, articular cartilage displays a very poor capacity for self-repair. Most of the cartilage injuries are maintained for years and may eventually lead to further degeneration.[2] Cartilage injuries affect both elderly and young populations. Nowadays, osteoarthritis is one of the major causes of disability among elderly people, whereas cartilage trauma is among the most common sports injuries in young adults.[3] Although many repair techniques have been proposed over recent decades, there is still no satisfactory method for successful regeneration of long-lasting robust hyaline cartilage tissue to replace the damaged cartilage.[4] The repair of articular cartilage remains one of the most challenging topics in orthopedic research.

Tissue engineering, which is an interdisciplinary science that combines the concepts of engineering and life science with isolated cells and scaffolds, may be a promising way to restore functional hyaline cartilage of joints.[5–8] Cells, scaffolds, and bioactive molecules are the three main elements of tissue engineering. The function of scaffolds is not only to accommodate the transplanted cells but also to guide new tissue formation and play an important role in maintaining the phenotype of chondrocytes.[9,10]

Synthesized scaffolds are widely used in cartilage tissue engineering due to their easier modification to meet diverse requirements, but there are still concerns about their biocompatibility and biodegradation. Naturally derived biological scaffolds are becoming more attractive and are wider applied for tissue engineering. Extracellular matrix (ECM) is the unique product of resident cells and contains entrapped bioactive molecules that interact with cells. The ECM is possibly nature's ideal biological scaffold material for individual tissues and organs.[11] Many ECM materials have been

[1]The Department of Orthopaedic Surgery, The Second Hospital of Shanxi Medical University, Taiyuan, P.R. China.
[2]School of Medicine, Dentistry, and Biomedical Sciences, Queen's University Belfast, Belfast, United Kingdom.
[3]The Shanxi Eye Hospital, Taiyuan, P.R. China.
[4]Orthopaedic Department, Xiehe Hospital, Tongji Medical Collage of Huazhong University of Science and Technology, Wuhan, P.R. China.
[5]Stem Cells and Regeneration Research Group, Department of Orthopaedics & Traumatology, Faculty of Medicine, Li Ka Shing Institute of Health Sciences, The Chinese University Hong Kong, Shatin, Hong Kong, P.R. China.

studied and applied for practical usage in tissue engineering. These include ECMs from the small intestine, skin, heart valve, and urinary bladder.[12–15] The application of decellularized ECM as a scaffold material may be especially beneficial to the damaged tissues, as it contains most of the structural and functional proteins of the original tissues.[11] Previous studies also showed that specific ECMs can promote the differentiation of embryonic stem cells into differentiated cells and structures that are similar to the tissue from which the matrix is derived and that the cartilage extract can promote the chondrogenesis of embryonic stem cells *in vitro*.[13]

The aim of this study was to fabricate and characterize a novel acellular cartilage matrix (ACM) and investigate the feasibility of using it as a scaffold in further cartilage tissue engineering studies.

Materials and Methods

Materials

Fresh bovine knee joints were obtained from a local abattoir. All the joints were transferred to the laboratory on ice within 2 h postsacrifice. Hyaline cartilage slices were dissected immediately; washed thoroughly in 4°C phosphate-buffered saline (PBS) containing 10 KU/mL Aprotinin (Sigma-Aldrich, Dorset, United Kingdom); and stored at −80°C for future use.

Fabrication of ACM scaffold

The cartilage slices were first immersed into liquid nitrogen for 5 min and then freeze-dried for 24 h at −56°C in a ChristTM Beta 1-8K lyophilizer (Christ, Osterode, Germany). The weight loss was calculated as $\Delta W\% = (W0 - W1)/W0 \times 100$, in which W0 represents the original weight of the sample and W1 represents the weight after the freeze-drying procedure. After the freeze-drying procedure, the samples were ground into a fine powder using a Rondol Freezer Mill 6850 (Rondol Technology, Staffordshire, United Kingdom) at a temperature of −196°C for 30 min.

The decellularization process was adopted from Mirsadraee *et al.*[16] and Grauss *et al.*[17] with minor modifications. Briefly, the cartilaginous powder was treated with 0.5% (w/v) trypsin/PBS solution for 24 h in a 37°C incubator with vigorous agitation. Fresh trypsin solution was changed every 4 h. The samples were then washed with PBS and treated in a nuclease solution (containing 50 U/mL deoxyribonuclease and 1 U/mL ribonuclease A in 10 mM Tris–HCl, pH 7.5) with agitation at 37°C for 4 h. After the nuclease digestion, the samples were treated with 10 mM hypotonic Tris–HCl solution for 20 h and then incubated in 1% Triton X-100 (v/v, in PBS) for 24 h. Finally, the samples were washed in PBS for six cycles of 8 h washing and stored at −80°C. During this process, 100 U/mL penicillin, 100 μg/mL streptomycin, and 2.5 μg/mL fungizone were included in all the above solutions. Aprotinin (10 KU/mL) was added into all solutions except those of trypsin and nuclease. All reagents were supplied by Sigma-Aldrich.

The ACM was put into cylindrical molds and freeze-dried at −56°C for 24 h to allow shape formation. The shaped ACM scaffolds were then carefully removed from the cylindrical molds and cross-linked by a 16 W ultraviolet (UV) light at 20 cm distance for 12 h. During the UV irradiation procedure, the ACM was turned over every 2 h. All the ACM scaffolds were sterilized using ethylene oxide and stored in sterile containers before use.

Histological evaluations

For histological evaluations, the ACM scaffolds were fixed in 4% paraformaldehyde in PBS (pH 7.2) for 12 h and decalcified in 15% ethylenediaminetetraacetic acid (EDTA) for 2 weeks. After washes in PBS, the samples were dehydrated in graded alcohols and then embedded in paraffin wax. Sections of 7 μm thickness were used for hematoxylin–eosin (H&E) staining and alcian blue staining, and this was done with the help of conventional procedures.

Immunohistochemical evaluations

For immunohistological evaluation of type II collagen, sections were dewaxed in xylene and brought to water via ethanol series of decreasing concentration. After three washes in PBS, sections were digested with Pronase K at 37°C for 15 min and pretreated with 3% hydrogen peroxide. The nonspecific binding of the antibody was blocked by applying 1:10 goat serum (Dako, Carpinteria, CA) diluted in PBS for 30 min. The sections were then incubated with 1:100 polyclonal mouse anti-rabbit type II collagen primary antibody (Merck, San Diego, CA) for 1 h at room temperature in a humidified incubation chamber. Sections were washed twice with PBS for 3 min and incubated with 1:100 biotinylated goat anti-mouse secondary antibody (Merck) for 30 min. After three PBS washes, streptavidin–horseradish peroxidase (1:100) was applied to the sections for 30 min. The sections were developed using a diaminobenzidine kit (Vector Laboratories, Burlingame, CA) for 10 min in the dark and then the reactions were stopped by tap water. Finally, the sections were counterstained with hematoxylin, cleared in xylene, and mounted with DPX. Normal rabbit articular cartilage sections were served as positive controls, and sections incubated with PBS instead of first antibody were served as negative controls.

Biochemical analysis

The glycosaminoglycan (GAG) and DNA content were quantified using a previously reported method.[15] Briefly, fresh cartilage slices and ACM were freeze-dried to constant weight and digested in a papain solution (125 μg/mL papain, 5 mm cysteine–HCl, and 5 mm EDTA in PBS) for 12 h in a water bath at 60°C. The solutions were cleared by centrifugation at 10,000 *g* for 30 min and stored at −80°C before testing.

GAG assay

The content of GAG was determined using a Blyscan glycosaminoglycan assay kit (Biocolor, Newtownabbey, United Kingdom). Briefly, 1 mL of 1,9-dimethylmethylene blue dye reagent was mixed with 100 μL samples and serially diluted standard solutions (chondroitin sulfate in the papain solution) by shaking at 240 rpm for 30 min, then the solutions

were centrifuged at 10,000 *g* for 10 min at 4°C to pellet the precipitate GAG–dye complex. After careful aspiration of the liquid, the pellets were dissolved in 1 mL of dissociation reagent. The absorbance was read in a GENios plate reader at 656 nm. The amount of GAGs was calculated by interpolation from a standard curve generated from serially diluted chondroitin sulfate standards in heat-inactivated papain solutions.

DNA assay

DNA was quantified using a PicoGreen DNA quantification kit (Molecular Probes, Eugene, OR) according to the manufacturer's instructions. Briefly, 10 μL of the papain digestion solutions of cartilage and ACM were mixed with 190 μL of PicoGreen solution. After 10 min of incubation in darkness, the samples were excited at 485 nm, and the fluorescence intensity at 520 nm was read on a GENios plate reader. The content of DNA was calculated by interpolation from a standard curve generated using serial dilutions of calf thymus DNA solubilized in heat-inactivated papain solutions.

pH stability tests

To test for pH stability, the blocks of 0.5×0.5×0.5 cm ACM scaffolds were placed at the centers of 100 mm culture dishes containing either PBS solution (pH 7.4) or complete culture medium. The pH of the solution was measured every 4 h at the middle of the ACM, at the edge of the ACM, and 5 mm from the ACM. A pH–time curve was generated by plotting the average of these three values against time.

Ultrastructural analysis

For scanning electron microscopy (SEM) examination, the ACM specimens were fixed by immersion into 2.5% glutaraldehyde (w/v in PBS solution) for 2 h, then washed with sodium dimethylarsenate buffer (pH 7.4), and postfixed by 1% osmium tetroxide (w/v). Each of the samples was dehydrated in an ascending ethanol series (30%, 50%, 70%, 90%, 95%, and 100%, v/v) for 10 min and dried at critical point. The dried specimens were sputter coated with gold before examination using a JSM scanning electron microscope (Jeol, Tokyo, Japan).

The microstructure of the prepared ACM scaffolds, including porosity, pore size, and pore distribution, was determined by a mercury intrusion porosimetry method using a Pascel 140/240 Porosimeter (CE Instrument, Wigan, United Kingdom) according to the manufacturer's instructions. Briefly, 75 mg materials were weighed, put into a clean sample tube, and infused with mercury under increasing pressure. The total porosity was calculated from the total intrusion volume, and the distribution of pore sizes was calculated using the Washburn equation.[18]

Isolation and cultivation of rabbit mesenchymal stem cells

Rabbit bone marrow mesenchymal stem cells (MSCs) were harvested and cultured *in vitro* based on established protocols.[18,19] Under general anesthesia of intravenous injection of sodium pentobarbital 30 mg/kg, the proximal hind legs of New Zealand White rabbits aged 4–6 months were shaved and swabbed with 75% ethanol. An 18-gauge myeloid biopsy needle with a 10 mL syringe prewetted by 1 mL heparin solution (1000 units/mL) was used to aspirate 5 mL bone marrow from both femurs. The bone marrow aspirate was gently loaded onto 3 mL LymphoprepTM (1.077 g/mL; Axis-Shield, Oslo, Norway) in a 15 mL centrifuge tube and centrifuged for 30 min at 1500 *g*. After centrifugation, the mononuclear cells were collected from the interface layer, washed twice with PBS, resuspended in standard culture medium (high-glucose Dulbecco's modified Eagle's medium [DMEM] containing 10% fetal bovine serum [FBS], 100 units/mL penicillin, 100 μg/mL streptomycin, and 2.5 μg/mL amphotericin B; all from Invitrogen, Paisely, United Kingdom), and seeded into T-75 flasks at a density of 1×10^5 cells/cm^2. The cells were cultured at 37°C in a humidified atmosphere with 5% CO_2. The medium was first changed on the seventh day of culture and thereafter twice a week. Nonadherent cells were removed from cultures by PBS washing during the medium change. At 80–90% confluence, the primary MSCs were washed with PBS and detached from the flasks with 0.25% trypsin/0.02% EDTA solutions (Invitrogen) and passaged into new flasks at a ratio of 1:3.

Contact cytotoxicity assay

Before the loading of cells, all of the ACM scaffolds were prewetted with complete culture medium. Briefly, the ACM scaffolds were put into six-well plates, and 200 μL of complete culture media was carefully dropped onto the scaffolds with a pipette. After 2 h, the media were removed and the prewetted ACM scaffolds were left in the plates. The third passage MSCs were detached from the flasks using trypsin/EDTA and washed with PBS. After centrifugation at 500 *g* for 5 min, the cells were resuspended in complete culture medium to a final concentration of 1×10^7 cells/mL. Cell suspensions (100 μL) were loaded onto the ACM scaffolds and allowed to attach for 1 h in an incubator before additional medium was added. During the cell loading process, the ACM scaffolds were inverted twice with sterile forceps to ensure the cells attached evenly on the scaffolds. Then the cell–ACM complexes were incubated at 37°C in 5% CO_2 for 7 days with medium changes every 3 days. During the incubation, the morphology of the cells around the ACM scaffolds was examined using an inverted phase contrast microscope (Olympus, Tokyo, Japan), and digital images were recorded daily. At day 7, the cell–ACM complexes were fixed in preparation for SEM, as previously described.

Quantitative extraction cytotoxicity assay

The extraction medium for the cytotoxicity assay was prepared using a previously described method.[20] To obtain serial extraction media, 100 mL basic medium (high-glucose DMEM without phenol red) containing 1, 0.1, and 0.01 g ACM scaffolds, respectively, was incubated at 37°C, 5% CO_2 for 72 h. Then the extraction media were cleared by centrifugation at 4°C, 4000 *g* for 15 min, filtered through a 0.75 μm sterile mesh filter, and stored at −20°C for future use. To make conditioned culture medium, 5% FBS, 100 U/mL

penicillin, 100 mg/mL streptomycin, and 2.5 μg/mL Fungizone were added fresh into the medium before the cytotoxicity assay.

The extraction cytotoxicity assay was carried out using a CytoTox 96® Non-Radioactive Cytotoxicity Assay kit (Promega, Madison, WI) according to the manufacturer's instructions with minor modifications. Briefly, rabbit MSCs of passage 3 were seeded into 24-well culture plates at the concentration of 1×10^4 cells/well and cultured in 1 mL standard culture medium in a humidified atmosphere at 37°C for 24 h. The cells were then incubated with a series 1 mL of conditioned medium, as prepared above, for 24, 48, and 72 h. Basic DMEM medium containing 5% FBS and antibiotics served as control. At each time point, the absorbance values of the medium and cell lysate were quantified at 492 nm using a GENios plate reader (Tecan, Theale, United Kingdom). The relative lactate dehydrogenase (LDH) release rate was calculated as % LDH Release = Medium A492/(Medium A492+Cell Lysate A492).

Cell proliferation assay

The effect of ACM on cell proliferation was evaluated using a cell proliferation Biotrak ELISA system (Amersham Biosciences, Buckinghamshire, United Kingdom). Briefly, MSCs of passage 3 were trypsinized and innoculated into 96-well plates at a density of 1×10^3 cells/well and cultured in standard culture medium at 37°C, 5% CO_2 for 24 h. The media were then changed to serial ACM-conditioned medium, as that which was described earlier. Cells were cultured for 3, 6, and 9 days. At each time point, the cells were washed with PBS and then labeled with bromodeoxyuridine (BrdU) for 2 h. After fixation, the cells were blocked and incubated with peroxidase-labeled anti-BrdU antibody for 90 min, which was followed by an incubation with tetramethylbenzidine (TMB) substrate at room temperature. When the required color intensity was achieved, the reactions were stopped with 1 M sulfuric acid, and the optical density was determined at 450 nm using a GENios plate reader.

Repair of cartilage defects with the MSC–ACM constructs

The ACM were cut into 5×5×5 mm blocks and sterilized using ethylene oxide for 8 h 1 day before the experiments. All of the ACM scaffolds were prewetted with complete culture medium before the loading of cells. The MSCs were resuspended in complete culture medium to a final concentration of 1×10^7 cells/mL. Then 100 μL of the cells were loaded onto the ACM scaffold and allowed to attach for 1 h in an incubator before additional medium was added. During the cell loading process, the ACM were turned over twice with a sterile forceps to make the cells distribute evenly on the ACM scaffold. The MSC–ACM constructs were cultured for an additional 24 h in an incubator with 5% CO_2 and 95% humidity at 37°C before the implantation.

Eight healthy adult male New Zealand White rabbits aged 4–6 months were used in this study. Four rabbits were used for the 6-week study, and four were used for the 12-week study. All the animal experiments were performed with the approval of the ethics committee of Shanxi Medical University of China and Queen's University Belfast, United Kingdom. All the surgical processes were conducted under sterile conditions.

The rabbits were general anesthetized, as previously described. The knee joints of both sides were shaved and swabbed with 75% ethanol. Medial incisions were applied over the joints and the patellae were dislocated laterally to expose the articular cartilage of the patella grooves. Full-thickness osteochondral defects (4 mm in diameter; 3 mm deep) were created in the weight-bearing area of patellar grooves on both knees using a hand drill with a blocking tube to control the depths of the defects. The defects were extending through all chondral layers into the subchondral bone plate. After the drilling, all the defects were rinsed with sterile physiological saline (0.9% NaCl, w/v) to remove the debris.

The eight defects created in four rabbits were randomly divided into two groups. In group A, the cartilage defects were filled with ACM scaffolds alone; in group B, the defects were filled with MSC–ACM constructs. The scaffolds and the MSC–ACM constructs were filled into the defects with a push-fit technique. All rabbits were kept in separate cages and were allowed to move freely after the surgery. At 6 and 12 weeks postoperation, four rabbits were sacrificed by overdose intravenous injection of sodium pentobarbital, and the knee joints were harvested for further examinations.

Evaluation of cartilage repair

After overall examination of the joints cavity and synovial membrane, the harvested joints were examined grossly under a surgical microscope to observe the surface of the regenerated tissues, the filling of the defects, and the interface healing between the repaired tissue and the adjacent normal cartilage. Macrographic evaluations were graded into three scales: complete repair, incomplete repair, and no repair. This was attained with the help of the criteria described in Table 1.

After the macrographic examination, the samples were washed with PBS, fixed in 4% paraformaldehyde for 1 week, and decalcified with 15% EDTA for 4 weeks at room temperature. After being thoroughly rinsed, the samples were dehydrated and embedded in paraffin. Sagittal sections of 7 μm thickness were used for H&E staining. The histological results were graded using a semiquantitative grading system modified from Wakitani *et al.*, as shown in Table 2. The histological grading was performed by two authors in a blind fashion.

Statistical analysis

All data were expressed as mean ± standard deviation and analyzed using the SPSS 13.0 software (SPSS, Chicago, IL). Student's *t*-test was used for biochemical assays, and analysis of variance (ANOVA) tests were used for quantitative extraction cytotoxicity assays and cell proliferation assays. Mann–Whitney *U*-test was used for analyzing the histological ranked score between groups. *p*-Values less than 0.05 were considered statistically significant.

Table 1. Macrographic Evaluation Criteria[58,59]

	Complete repair	*Incomplete repair*	*No repair*
Surface	Smooth	Irregular	Disruptive
Filling	>90%	60–89%	<59%
Thickness	>2/3	1/3–2/3	<1/3

Table 2. Semiquantitative Histological Grading Scores for Cartilage Repair

Category	*Points*
Cell morphology	
Hyaline cartilage	0
Mostly hyaline cartilage	1
Mostly fibrocartilage	2
Mostly noncartilage	3
Noncartilage only	4
Matrix staining	
Normal (compared with host adjacent cartilage)	0
Slightly reduced	1
Markedly reduced	2
No metachromatic stain	3
Surface regularity	
Smooth (>3/4)	0
Moderate (1/2–3/4)	1
Irregular (1/4–1/2)	2
Severely irregular (<1/4)	3
Thickness of cartilage	
>2/3	0
1/3–2/3	1
<1/3	2
Integration of donor with host adjacent cartilage	
Both edges integrated	0
One edge integrated	1
Neither edge integrated	2
Total maximum	14

Modified from the scale described by Wakitani *et al.*[60] and Hiraide *et al.*[61]

Results

General observation, histological and immunohistochemical evaluations

Fresh cartilage slices were bluish and hyaline-like, but after the freeze-dry procedure they lost water contents and turned into dry, white slices. The average weight loss was about 85–90%, varying between different experiments. After the freeze-grinding procedure, all cartilage slices were ground into fine white powder. The ACM formed sponge-like porous scaffolds after the freeze-drying procedure. After cross-linking by UV irradiation, the ACM scaffolds looked slightly yellowish but maintained their shape and structure (Fig. 1A).

For histological analysis, H&E staining showed that the ACM scaffolds were composed of red-stained, irregular-shaped cartilaginous particles with a rough surface topography. There were fiber-like structures connecting the particles to form a net-like structure (Fig. 1B). Sections stained with alcian blue had a blue appearance, indicating that the ACM scaffolds contained GAG. Cartilage lacunae were clearly visible on the cartilaginous particles, and there were no chondrocytes or cell fragments present in the lacunae (Fig. 1C).

The cartilaginous particles demonstrated a positive brown staining when immunostained for type II collagen, indicating that the ACM scaffolds retained the type II collagen component after the decellularization procedure (Fig. 1D).

Biochemical analysis

The DNA assay showed that the amounts of DNA per mg dry weight of the cartilage powder before and after the decellularization procedure were $2.23 \pm 0.52\,\mu g/mg$ and $0.03 \pm 0.01\,\mu g/mg$, respectively. There was a highly significant reduction in the DNA content after the decellularization procedure (t-test; $n = 5$, $p < 0.01$, Fig. 2A).

The GAG assay showed that the amounts of GAG per mg dry weight of the cartilage powder before and after the decellularization procedure were $47.81 \pm 7.19\,\mu g/mg$ and $41.69 \pm 9.43\,\mu g/mg$, respectively. There was no statistically significant difference between the two groups before and after the decellularization procedure (t-test; $n = 5$, $p > 0.05$, Fig. 2B).

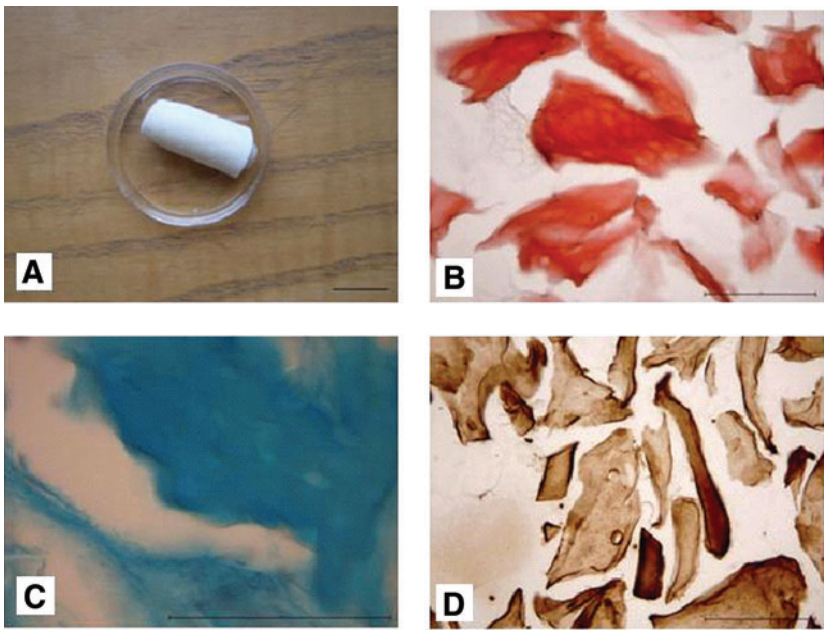

FIG. 1. Macroscopic and microscopic appearance of acellular cartilage matrix (ACM). (**A**) Macroscopic appearance, (**B**) hematoxylin–eosin staining, (**C**) alcian blue staining, (**D**) immunohistology of collagen II. Scale bar: (**A**) 10 mm and (**B–D**) 100 μm. Color images available online at www.liebertonline.com/ten.

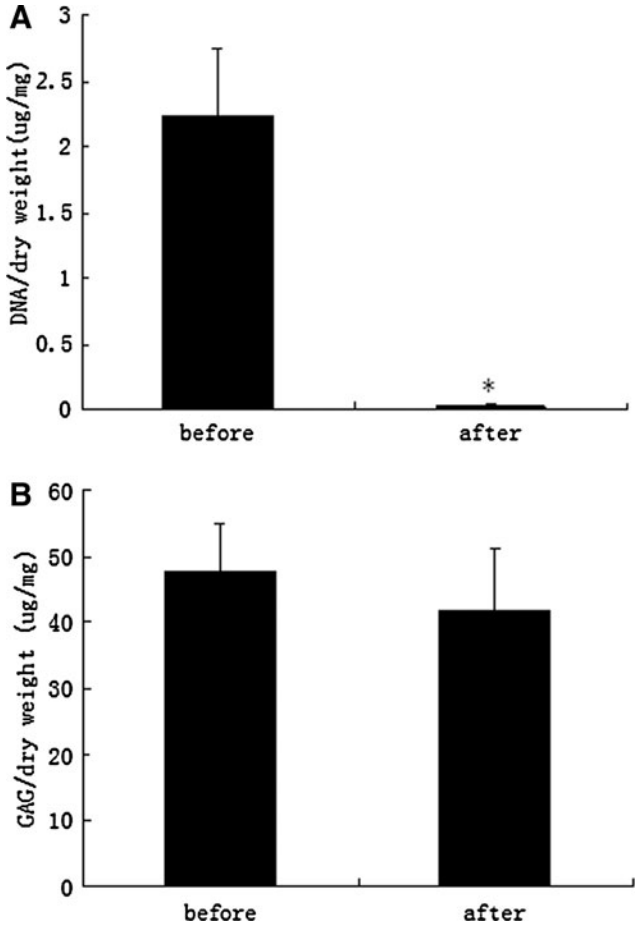

FIG. 2. Biochemical assay of ACM before and after the decellularization procedure. (**A**) DNA content and (**B**) GAG content. $^*p < 0.05$. GAG, glycosaminoglycan.

pH stability tests

Continuous monitoring of pH changes indicated pH stability for ACM scaffolds placed in both PBS and complete culture medium for all time points investigated. The average pH values were within the physiologic range of 7.2–7.4.

Microstructural analysis

SEM analysis demonstrated that ACM scaffolds had a spongy appearance with uniformly distributed pores and high interconnection between the macroporous structures (Fig. 3A). The diameters of most pores ranged between 30 and 150 μm (Fig. 3B).

The microstructure of the ACM scaffold, including porosity, pore size, and pore distribution, was determined using mercury intrusion porosimetry method.[18] The results revealed that the average total porosity of the ACM scaffolds was 89.37%, the average pore diameter was 90.8 μm, and the bulk density was 0.38 g/cm^2. The pore size distribution analysis showed that over 80% of the scaffold volumes had been formed by pores ranging from 20 to 100 μm, indicating that the ACM scaffolds were highly porous and that they had a wide distribution of pore sizes.

Contact cytotoxicity assay

The contact cytotoxicity assay showed that rabbit MSCs grew well on the ACM scaffolds. Also, there were no apparent morphological changes to the cells adjacent to the ACM scaffolds. These cells were similar in appearance to the control cells cultured in standard medium without ACM. Some cells adjacent to the ACM gradually attached to the ACM and formed cell aggregates (Fig. 3C). SEM showed that MSCs were distributed evenly over the surface of the ACM.

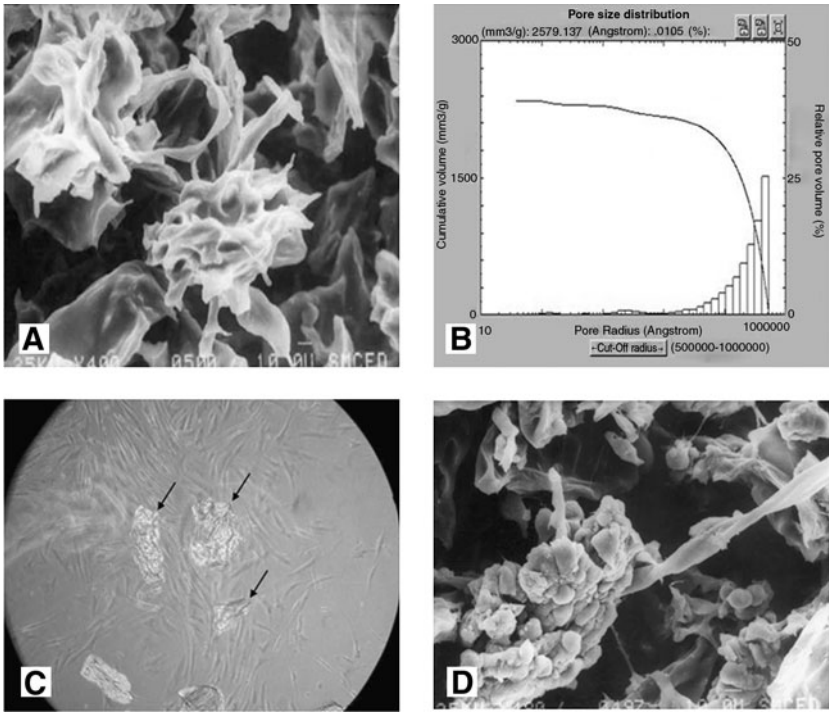

FIG. 3. Microstructure of ACM. (**A**) Scanning electronic microscopy scanning of ACM (scale bar: 10 μm), (**B**) pore size distribution of ACM, (**C**) contact cytotoxicity of ACM, showing the ACM particle (arrows) with surrounding cells, inverted microscopy ×100, and (**D**) scanning electronic microscopy scanning ×400.

The cells covered most of the pores with good attachment, indicating good biocompatibility of the ACM materials (Fig. 3D).

Quantitative extraction cytotoxicity assay

For the extract cytotoxicity assay, MSCs were cultured in conditioned medium with different concentrations of the ACM extract. No statistical differences were detected for cell viability between ACM-conditioned medium and control medium or between different concentrations of conditioned medium (ANOVA, $p > 0.05$, Fig. 4A).

Cell proliferation assay

The proliferation assay of MSCs cultured with serial concentrations of ACM extraction showed that there was no statistical difference at days 0 and 3 among all the groups, whereas there was a significant increase in cell proliferation in the 10 mg/mL group at days 6 and 9 when compared with the other groups (ANOVA, $n = 6$, $p < 0.01$, Fig. 4B).

Evaluation of cartilage repairing

All of the rabbits survived the follow-up period with no signs of major wound infection, limited range of motion, or synovitis in the operated joints. All the rabbits regained their normal gaits and locomotion 1 week after the surgery.

The macrographic examination showed that there were no abrasions on the surrounding articular cartilage surfaces and no inflammation of the synovial membranes. Both the macrographic and the histological results showed that the experimental group (group A) achieved better repair than the control group both at 6 and 12 weeks (Fig. 5A–H and Table 3).

The histological grading scores in the experimental group were significantly better than those of the control group ($n = 4$, $p < 0.05$) both at 6 and 12 weeks. At the two time points tested, there was no difference for the control group, but there was a significant decrease of histological scores (sign of improvement of cartilage quality) in the experimental group, indicating that the repair of cartilage at 12 weeks was significantly better than at 6 weeks in the experimental group (Fig. 6).

Discussion

Despite the numerous approaches that have been developed to repair cartilage injuries over past decades, there is still no satisfactory method to regenerate long-lasting and functional hyaline cartilage tissue.[4] The repair of articular cartilage remains one of the most challenging topics in orthopedic research. Tissue engineering, which combines isolated cells with scaffolds to regenerate damaged tissue, has recently demonstrated tremendous clinical potential for regeneration of hyaline-like cartilage tissue for treatment of cartilage injuries.[5–8]

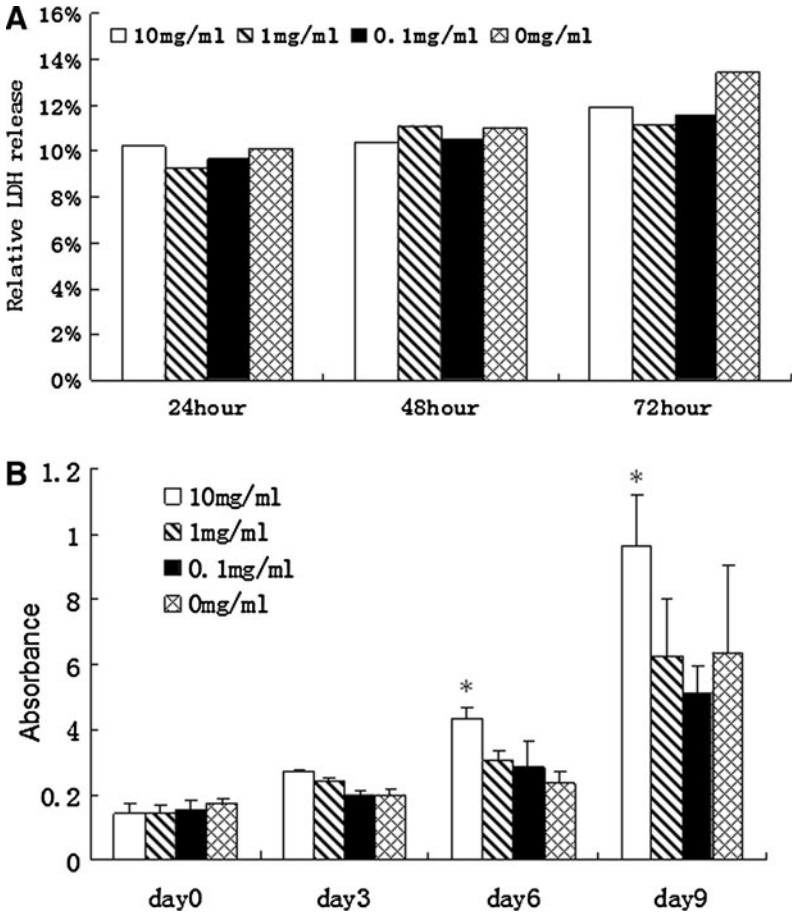

FIG. 4. (**A**) Quantitative extraction cytotoxicity assay of ACM between different concentrations of ACM extraction-conditioned medium. (**B**) Cell proliferation assay of MSCs cultured in different concentrations of ACM-conditioned medium (*$p < 0.01$). MSCs, mesenchymal stem cells.

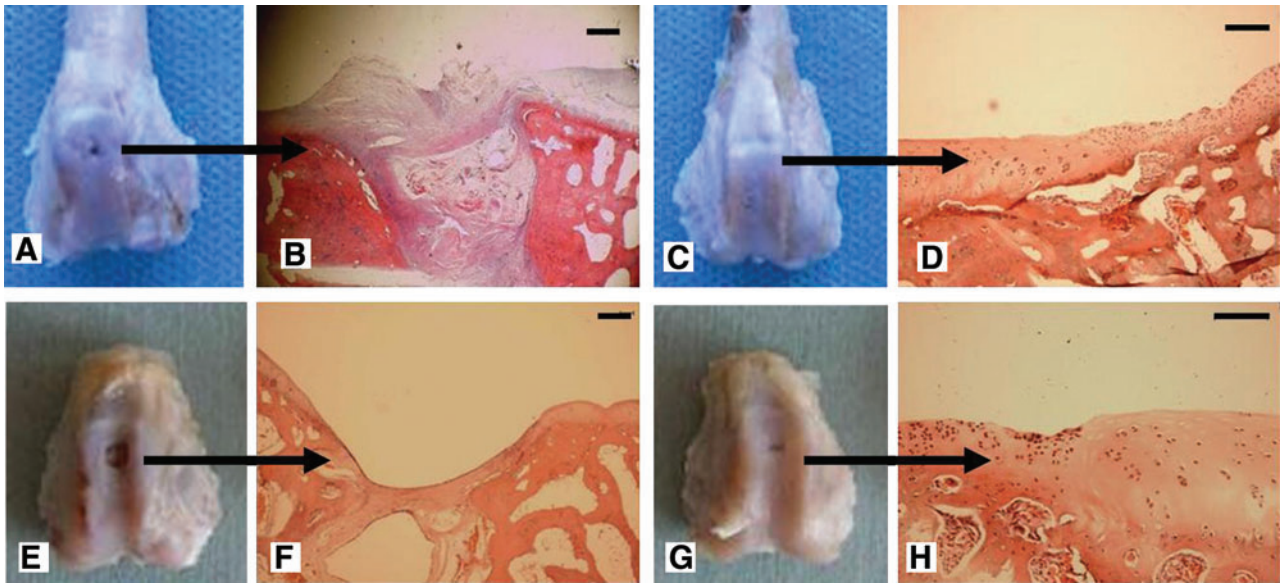

FIG. 5. Representative macrographs of knee joint samples. (**A**) Group A (scaffolds alone) at 6 weeks, (**C**) group B (scaffolds with MSCs) at 6 weeks, (**E**) group A (scaffolds alone) at 12 weeks, and (**G**) group B (scaffolds with MSCs) at 12 weeks. Representative histological sections of the cartilage defect areas. (**B**) Group A (scaffolds alone) at 6 weeks, (**D**) group B (scaffolds with MSCs) at 6 weeks, (**F**) group A (scaffolds alone) at 12 weeks, and (**H**) group B (scaffolds with MSCs) at 12 weeks. Scale bars = 100 μm. Color images available online at www.liebertonline.com/ten.

The three basic elements in tissue engineering are cells, scaffolds, and bioactive molecules. In cartilage tissue engineering, scaffolds play an important role not only in the delivery and retention of cells in cartilage defects but also in maintaining the chondrocyte phenotype.[9,10]

Scaffolds applied in tissue engineering can be divided into two categories: synthesized scaffolds such as poly glycolic acid,[21] poly(l-lactic acid),[22] poly(l-lactic-co-glycolic acid),[23] and polyethylene oxide[24] and naturally derived scaffolds such as agarose,[25] alginate,[26] chitosan,[27] hyaluronic acid,[28] gelatin,[29] fibrin glue,[30,31] and collagen derivatives.[32,33] Generally, the ideal biomaterial should be nontoxic, biocompatible, able to promote favorable cellular interactions and tissue development, and possess adequate mechanical and physical properties.[34] With regard to synthesized scaffolds, it is relatively easy to modify their physical, chemical, and mechanical characteristics and degeneration profile to meet the requirements of various applications. However, they have disadvantages of poor biocompatibility, and their acid metabolism byproducts may inhibit the growth of cells. Hence, more researchers have turned their attention to naturally derived scaffolds due to their superior biocompatibility and biodegradability.

ECM is the product of the resident cells of tissues and it serves both structural and functional roles.[35] Using ECM as scaffold material provides great advantages of biocompatibility and biodegradability, as ECM is a product of the resident cells and thus may interact with the cells.[11] The main components of ECM are structural proteins such as collagen and adhesive molecules such as GAGs, proteoglycans, and glycoproteins.[35] Since these components are generally con-

Table 3. Macrographic Evaluation of the Cartilage Repair

	6 Weeks		*12 Weeks*	
	Group A	*Group B*	*Group A*	*Group B*
Complete repair	0	1	0	2
Incomplete repair	1	2	1	2
No repair	3	1	3	0
Total	4	4	4	4

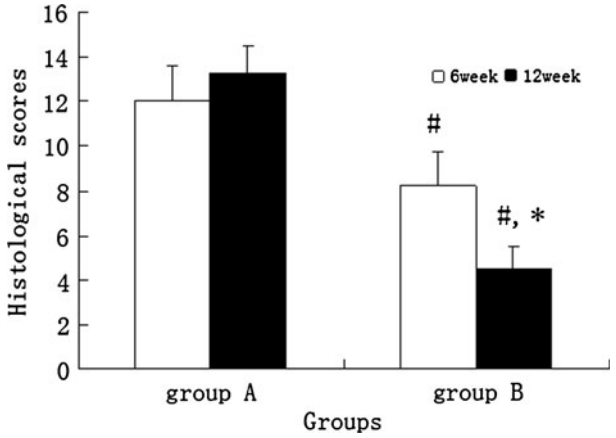

FIG. 6. Histological scores of the cartilage repair in the two experimental groups at 6 and 12 weeks. $^{\#}p < 0.05$ compared with group A and $^{*}p < 0.05$ compared with the group at 6 weeks.

served among species, ECM can be used for allogeneic transplantation with good tolerance and even for xenogenetic recipients.[36] Also, ECM can provide not only physical support to the cells but also biological signals. Research has showed that many bioactive molecules are resident in ECM, including transforming growth factor-β, basic fibroblast growth factor, epidermal growth factor, vascular epidermal growth factor, hepatocytes growth factor, and platelet-derived growth factor.[35] These bioactive molecules are admixed with binding molecules such as decorin and biglycan. Despite being in extremely small quantities, these molecules act as potent modulators of cell behavior.[35] As each ECM contains unique components relevant to its location, it is possible that tissue specific matrices can promote the repair of their original tissues or organs. In a study of the function of ECM, Philp *et al.* found that the matrices of cartilage could promote the chondrogenesis of embryonic stem cells.[37]

Nowadays, there are many successful reports on using decellularized ECMs as scaffolds for tissue repair. For example, the ECMs from skin,[38–40] small intestinal submucosa,[41–43] urinary bladder,[15,44,45] heart valves,[12,16,46] nerves,[47–49] and tendons[50,51] have been studied for tissue engineering applications with promising results. In this study, our aim was to fabricate and characterize a novel ACM as a scaffold for cartilage tissue engineering.

Cartilage is a dense tissue with sparsely distributed chondrocytes embedded in a vast ECM. Compared with other tissues such as small intestine, bladder, or heart valves, it is difficult to decellularize cartilage. To fully remove the chondrocytes and cell fragments from the matrix, solutions should be able to permeate throughout the matrix. So as a first step, we freeze-dried cartilage slices and ground the cartilage into fine powder. This greatly increased the surface area of the material and reduced the distance for the permeation of chemicals and enzymes. In the following decellularization stage, we employed a protocol adopted from Mirsadraee *et al*.[16] and Grauss *et al*.[17] with minor modifications. This decellularization process included an enzymatic digestion procedure with trypsin and nuclease, an osmotic lysis procedure with a hypotonic solution, and a detergent treatment procedure of Triton ×100. Protease inhibitors were added in all steps except the enzyme digestion step to prevent autolysis of the proteins. Although some researchers reported successful decellularization using only trypsin digestion or Triton ×100 detergent treatment,[52–54] other studies showed that treatment with trypsin or Triton alone may not totally remove the cells and cell fragments from the matrix.[14] In this study, a procedure combining enzymatic digestion, hypotonic lysis, and detergent treatments was employed to achieve the best decellularization results. After the decellularization procedure, histological analysis showed that there were no cells or cell fragments left in the matrix. The DNA content assay confirmed this result, indicating an extremely low level of DNA detected in the ACM samples after the decellularization procedure.

In this study, the ACM sections were stained with alcian blue for the detection of GAG and immunologically stained for the detection of type II collagen. The results showed that the ACM retained these two major components of cartilage, indicating that the decellularization procedure had little effect on the biochemical components of the cartilaginous matrix. This retention of cartilaginous components was also confirmed by the quantitative biochemical analysis of the ACM, which showed that there was no statistically significant difference between the fresh cartilage slices and the ACM scaffolds for GAG content.

The microstructure of a scaffold is also important in cell–scaffold interactions. Studies showed that the pores in the scaffolds are necessary for cell anchorage and proliferation. Also, the pores in the scaffolds greatly increase the surface area for nutrition and waste exchange, improving the mechanical interlocking between the implant and the host tissues.[55] In this study, the SEM examination showed that the ACM had a sponge-like appearance with uniformly distributed pores with high interconnection between the macroporous structures. The porosity assay showed that the ACM had a relatively high porosity of about 89%. These microstructural characteristics imply that the ACM scaffold may be a good candidate scaffold for cartilage tissue engineering.

Compared with the synthesized scaffolds, naturally derived scaffolds usually have lower mechanical strength and higher rates of degradation. To improve the mechanical stiffness and decrease the degradation rate, it is often necessary to use cross-linking techniques to modify scaffold properties. Many chemical reagents such as glutaraldehyde, isocyanates, alcohol, formaldehyde, and imidoesters have been applied for the cross-linking of scaffolds; however, their effectiveness may be compromised by the increasing cytotoxicity and decreasing biocompatibility related to the residual of chemicals.[56] UV irradiation can cross-link the collagen fibers by producing free radicals on tyrosine and phenylalanine residues and unlike chemical cross-linking methods, there are no concerns about residuals.[57] To eliminate the side effects of chemical cross-linking, in this study we employed a nonchemical cross-linking method of UV irradiation.[56] In the biocompatibility testing, we used both a contact cytotoxicity assay and an extract cytotoxicity assay. Results showed that the ACM had good biocompatibility with rabbit MSCs and that there was no sign of cytotoxicity on MSCs, suggesting that UV irradiation is an approprate alternative to chemical cross-linking.

The ACM powders were transformed into cylindrical shape by freeze-dry and UV irradiation cross-linking. In our preliminary experiments, we tested various irradiation times for cross-linking and found that 12 h is the optimal time in this study. We did not purposely test the effects of ACM concentrations and pore sizes on mechanical stiffness of ACM, because the purpose of developing this ACM scaffold was to hold the MSCs and provide a bridging scaffold to fill the cartilage defect. It is not our purpose to develop a mechanically strong (e.g., strong scaffold as cartilage) ACM to replace cartilage. The main function of this ACM construct is to provide a scaffolding and a suitable microenvironment for MSCs to differentiate into chondrocytes and form cartilage matrices. The reasons behind making the ACM powders into cylindrical shape is mainly for easy handling of the biomaterials, to allow the cells to seed into it more evenly, and to fill the defect gap quickly during the surgery. The animal experimental data have demonstrated that the ACM scaffolding has promoted cartilage defect repair and that it could be a good alternative biomaterial for cartilage repair.

Interestingly, in this study, in addition to the good biocompatibility demonstrated with cultured MSCs, the ACM showed a trend of improving the proliferation of the MSCs. When cultured in the ACM-conditioned medium, MSCs showed no signs of growth inhibition regardless of the concentration of ACM. In the conditioned medium prepared from 10 mg/mL ACM, the cells showed a significant increase of proliferation at days 6 and 9. This result indicates that the ACM had no inhibitory effect on the growth of MSCs and that higher concentration promoted bone marrow MSC proliferation. One of the possible reasons for this enhanced proliferation may be associated with growth factors or bioactive molecules entrapped in the ACM,[35] but the exact mechanisms of this phenomenon require further investigation.

In this study, we used this novel ACM as a scaffold for the repair of experimental cartilage defects. The results showed that the transplantation of MSC–ACM constructs improved the repair of cartilage defects, as there were some levels of repair even in the control group in which the defects were filled only with the ACM. The ACM scaffold filled in defects may act as a bridging scaffold and maintain some bone marrow MSCs (limited numbers) that had leaked into the defects after the drilling. But the experimental group (ACM with MSCs) achieved much better cartilage repair quality than the control group, indicating the importance of presence of enough cartilage progenitor (repair) cells in cartilage tissue engineering. After 12 weeks of implantation, no ACM residue was found in the defects, thus implying good biodegradability of this scaffold.

Conclusions

In this study, a novel ACM was developed as a potential scaffold for cartilage tissue engineering. The histological and biochemical studies showed that the ACM retains the major hyaline cartilage ECM tissue components of type II collagen and GAG. The microstructural study revealed that the ACM has a sponge-like porous structure with a suitable pore size for cell attachment. The cytotoxicity and proliferation assays demonstrated that the ACM has good biocompatibility characteristics which may promote the proliferation of MSCs. The *in vivo* animal experimental work demonstrated that the ACM can be used as a scaffold for MSCs and that the combination of ACM and MSCs has significantly improved cartilage repair. Taken together, our results indicate that ACM may be an appropriate biocompatible scaffold for use in cartilage tissue engineering.

Acknowledgments

This study was supported by the Overseas Research Studentship from Universities UK and Queens University Belfast to Ziquan Yang and Gang Li.

Disclosure Statement

No conflict of interests is declared by all the authors.

References

1. Hunziker, E.B. Articular cartilage repair: basic science and clinical progress. A review of the current status and prospects. Osteoarthritis Cartilage **10,** 432, 2002.
2. O'Driscoll, S.W. The healing and regeneration of articular cartilage. J Bone Joint Surg Am **80,** 1795, 1998.
3. Steinert, A.F., Ghivizzani, S.C., Rethwilm, A., Tuan, R.S., Evans, C.H., and Noth, U. Major biological obstacles for persistent cell-based regeneration of articular cartilage. Arthritis Res Ther **9,** 213, 2007.
4. Redman, S.N., Oldfield, S.F., and Archer, C.W. Current strategies for articular cartilage repair. Eur Cell Mater **9,** 23, 2005.
5. Brittberg, M., Lindahl, A., Nilsson, A., Ohlsson, C., Isaksson, O., and Peterson, L. Treatment of deep cartilage defects in the knee with autologous chondrocyte transplantation. N Engl J Med **331,** 889, 1994.
6. Kafienah, W., Mistry, S., Dickinson, S.C., Sims, T.J., Learmonth, I., and Hollander, A.P. Three-dimensional cartilage tissue engineering using adult stem cells from osteoarthritis patients. Arthritis Rheum **56,** 177, 2007.
7. Kuo, C.K., Li, W.J., Mauck, R.L., and Tuan, R.S. Cartilage tissue engineering: its potential and uses. Curr Opin Rheumatol **18,** 64, 2006.
8. Wang, Y., Blasioli, D.J., Kim, H.J., Kim, H.S., and Kaplan, D.L. Cartilage tissue engineering with silk scaffolds and human articular chondrocytes. Biomaterials **27,** 4434, 2006.
9. Hauselmann, H.J., Fernandes, R.J., Mok, S.S., Schmid, T.M., Block, J.A., and Aydelotte, M.B. Phenotypic stability of bovine articular chondrocytes after long-term culture in alginate beads. J Cell Sci **107 (Pt 1),** 17, 1994.
10. Kimura, T., Yasui, N., Ohsawa, S., and Ono, K. Chondrocytes embedded in collagen gels maintain cartilage phenotype during long-term cultures. Clin Orthop Relat Res **186,** 231, 1994.
11. Badylak, S.F. The extracellular matrix as a biologic scaffold material. Biomaterials **28,** 3587, 2007.
12. Mirsadraee, S., Wilcox, H.E., Watterson, K.G., Kearney, J.N., Hunt, J., and Fisher, J. Biocompatibility of acellular human pericardium. J Surg Res **143,** 407, 2007.
13. Jin, C.Z., Park, S.R., Choi, B.H., Park, K., and Min, B.H. *In vivo* cartilage tissue engineering using a cell-derived extracellular matrix scaffold. Artif Organs **31,** 183, 2007.
14. Meyer, S.R., Chiu, B., Churchill, T.A., Zhu, L., Lakey, J.R., and Ross, D.B. Comparison of aortic valve allograft decellularization techniques in the rat. J Biomed Mater Res A **79,** 254, 2006.
15. Bolland, F., Korossis, S., Wilshaw, S.P., Ingham, E., Fisher, J., and Kearney, J.N. Development and characterisation of a full-thickness acellular porcine bladder matrix for tissue engineering. Biomaterials **28,** 1061, 2007.
16. Mirsadraee, S., Wilcox, H.E., Korossis, S.A., Kearney, J.N., Watterson, K.G., and Fisher, J. Development and characterization of an acellular human pericardial matrix for tissue engineering. Tissue Eng **12,** 763, 2006.
17. Grauss, R.W., Hazekamp, M.G., Oppenhuizen, F., van Munsteren, C.J., Gittenberger-de Groot, A.C., and DeRuiter, M.C. Histological evaluation of decellularised porcine aortic valves: matrix changes due to different decellularisation methods. Eur J Cardiothorac Surg **27,** 566, 2005.
18. Joschek, S., Nies, B., Krotz, R., and Goferich, A. Chemical and physicochemical characterization of porous hydroxyapatite ceramics made of natural bone. Biomaterials **21,** 1645, 2000.
19. Shao, X.X., Hutmacher, D.W., Ho, S.T., Goh, J.C., and Lee, E.H. Evaluation of a hybrid scaffold/cell construct in repair of high-load-bearing osteochondral defects in rabbits. Biomaterials **27,** 1071, 2006.

20. Cehreli, M.C., Sahin, S., Ergunay, K., Ustacelebi, S., and Sevil, U.A. Cytotoxicity of eluates from a gamma-ray-polymerized poly(methyl methacrylate). J Biomater Appl **18,** 223, 2004.
21. Mahmoudifar, N., and Doran, P.M. Tissue engineering of human cartilage in bioreactors using single and composite cell-seeded scaffolds. Biotechnol Bioeng **91,** 338, 2005.
22. Ushida, T., Furukawa, K., Toita, K., and Tateishi, T. Three-dimensional seeding of chondrocytes encapsulated in collagen gel into PLLA scaffolds. Cell Transplant **11,** 489, 2002.
23. Chen, G., Sato, T., Ushida, T., Hirochika, R., Shirasaki, Y., and Ochiai, N. The use of a novel PLGA fiber/collagen composite web as a scaffold for engineering of articular cartilage tissue with adjustable thickness. J Biomed Mater Res A **67,** 1170, 2003.
24. Subramanian, A., Vu, D., Larsen, G.F., and Lin, H.Y. Preparation and evaluation of the electrospun chitosan/PEO fibers for potential applications in cartilage tissue engineering. J Biomater Sci Polym Ed **16,** 861, 2005.
25. Mauck, R.L., Yuan, X., and Tuan, R.S. Chondrogenic differentiation and functional maturation of bovine mesenchymal stem cells in long-term agarose culture. Osteoarthritis Cartilage **14,** 179, 2006.
26. Ma, H.L., Chen, T.H., Low-Tone, Ho, L., and Hung, S.C. Neocartilage from human mesenchymal stem cells in alginate: implied timing of transplantation. J Biomed Mater Res A **74,** 9, 2005.
27. Di Martino, A., Sittinger, M., and Risbud, M.V. Chitosan: a versatile biopolymer for orthopaedic tissue-engineering. Biomaterials **26,** 5983, 2005.
28. Yoo, H.S., Lee, E.A., Yoon, J.J., and Park, T.G. Hyaluronic acid modified biodegradable scaffolds for cartilage tissue engineering. Biomaterials **26,** 1925, 2005.
29. Chang, C.H., Kuo, T.F., Lin, C.C., Chou, C.H., Chen, K.H., and Lin, F.H. Tissue engineering-based cartilage repair with allogenous chondrocytes and gelatin-chondroitin-hyaluronan tri-copolymer scaffold: a porcine model assessed at 18, 24, and 36 weeks. Biomaterials **27,** 1876, 2006.
30. Westreich, R., Kaufman, M., Gannon, P., and Lawson, W. Validating the subcutaneous model of injectable autologous cartilage using a fibrin glue scaffold. Laryngoscope **114,** 2154, 2004.
31. Dare, E.V., Vascotto, S.G., Carlsson, D., Hincke, M.T., and Griffith, M. Differentiation of a fibrin gel encapsulated chondrogenic cell line. Int J Artif Organs **30,** 619, 2007.
32. Freyria, A.M., Cortial, D., Ronziere, M.C., Guerret, S., and Herbage, D. Influence of medium composition, static and stirred conditions on the proliferation of and matrix protein expression of bovine articular chondrocytes cultured in a 3-D collagen scaffold. Biomaterials **25,** 687, 2004.
33. O Halloran, D.M., Collighan, R.J., Griffin, M., and Pandit, A.S. Characterization of a microbial transglutaminase cross-linked type II collagen scaffold. Tissue Eng **12,** 1467, 2006.
34. Mano, J.F., Silva, G.A., Azevedo, H.S., Malafaya, P.B., Sousa, R.A., and Silva, S.S. Natural origin biodegradable systems in tissue engineering and regenerative medicine: present status and some moving trends. J R Soc Interface **4,** 999, 2007.
35. Badylak, S.F. Regenerative medicine and developmental biology: the role of the extracellular matrix. Anat Rec B New Anat **287,** 36, 2005.
36. Gilbert, T.W., Sellaro, T.L., and Badylak, S.F. Decellularization of tissues and organs. Biomaterials **27,** 3675, 2006.
37. Philp, D., Chen, S.S., Fitzgerald, W., Orenstein, J., Margolis, L., and Kleinman, H.K. Complex extracellular matrices promote tissue-specific stem cell differentiation. Stem Cells **23,** 288, 2005.
38. Wise, J.B., Cabiling, D., Yan, D., Mirza, N., and Kirschner, R.E. Submucosal injection of micronized acellular dermal matrix: analysis of biocompatibility and durability. Plast Reconstr Surg **120,** 1156, 2007.
39. Chen, R.N., Ho, H.O., Tsai, Y.T., and Sheu, M.T. Process development of an acellular dermal matrix (ADM) for biomedical applications. Biomaterials **25,** 2679, 2004.
40. Feng, X., Shen, R., Tan, J., Chen, X., Pan, Y., and Ruan, S. The study of inhibiting systematic inflammatory response syndrome by applying xenogenic (porcine) acellular dermal matrix on second-degree burns. Burns **33,** 477, 2007.
41. Zhang, L., Liu, Z., Cui, P., Zhao, D., and Chen, W. SIS with tissue-cultured allogenic cartilages patch tracheoplasty in a rabbit model for tracheal defect. Acta Otolaryngol **127,** 631, 2007.
42. Le Visage, C., Yang, S.H., Kadakia, L., Sieber, A.N., Kostuik, J.P., and Leong, K.W. Small intestinal submucosa as a potential bioscaffold for intervertebral disc regeneration. Spine **31,** 2423, 2006.
43. Fox, D.B., Cook, J.L., Arnoczky, S.P., Tomlinson, J.L., Kuroki, K., and Kreeger, J.M. Fibrochondrogenesis of free intraarticular small intestinal submucosa scaffolds. Tissue Eng **10,** 129, 2004.
44. Obara, T., Matsuura, S., Narita, S., Satoh, S., Tsuchiya, N., and Habuchi, T. Bladder acellular matrix grafting regenerates urinary bladder in the spinal cord injury rat. Urology **68,** 892, 2006.
45. Kaya, M., Baba, F., Bolukbas, F., Boleken, M.E., Kanmaz, T., and Yucesan, S. Use of homologous acellular dermal matrix for abdominal wall reconstruction in rats. J Invest Surg **19,** 11, 2006.
46. Tudorache, I., Cebotari, S., Sturz, G., Kirsch, L., Hurschler, C., and Hilfiker, A. Tissue engineering of heart valves: biomechanical and morphological properties of decellularized heart valves. J Heart Valve Dis **16,** 567, 2007.
47. Neubauer, D., Graham, J.B., and Muir, D. Chondroitinase treatment increases the effective length of acellular nerve grafts. Exp Neurol **207,** 163, 2007.
48. Hudson, T.W., Zawko, S., Deister, C., Lundy, S., Hu, C.Y., and Lee, K. Optimized acellular nerve graft is immunologically tolerated and supports regeneration. Tissue Eng **10,** 1641, 2004.
49. Hudson, T.W., Liu, S.Y., and Schmidt, C.E. Engineering an improved acellular nerve graft via optimized chemical processing. Tissue Eng **10,** 1346, 2004.
50. Ingram, J.H., Korossis, S., Howling, G., Fisher, J., and Ingham, E. The use of ultrasonication to aid recellularization of acellular natural tissue scaffolds for use in anterior cruciate ligament reconstruction. Tissue Eng **13,** 1561, 2007.
51. Cartmell, J.S., and Dunn, M.G. Effect of chemical treatments on tendon cellularity and mechanical properties. J Biomed Mater Res **49,** 134, 2000.
52. Cebotari, S., Mertsching, H., Kallenbach, K., Kostin, S., Repin, O., and Batrinac, A. Construction of autologous human heart valves based on an acellular allograft matrix. Circulation **106 (Suppl 1),** I63, 2002.
53. Steinhoff, G., Stock, U., Karim, N., Mertsching, H., Timke, A., and Meliss, R.R. Tissue engineering of pulmonary heart valves on allogenic acellular matrix conduits: *in vivo* restoration of valve tissue. Circulation **102 (Suppl 3),** III50, 2000.
54. Kim, W.G., Park, J.K., and Lee, W.Y. Tissue-engineered heart valve leaflets: an effective method of obtaining acellularized valve xenografts. Int J Artif Organs **25,** 791, 2002.

55. Karageorgiou, V., and Kaplan, D. Porosity of 3D biomaterial scaffolds and osteogenesis. Biomaterials **26,** 5474, 2005.
56. Lew, D.H., Liu, P.H., and Orgill, D.P. Optimization of UV cross-linking density for durable and nontoxic collagen GAG dermal substitute. J Biomed Mater Res B Appl Biomater **82,** 51, 2007.
57. Weadock, K.S., Miller, E.J., Bellincampi, L.D., Zawadsky, J.P., and Dunn, M.G. Physical crosslinking of collagen fibers: comparison of ultraviolet irradiation and dehydrothermal treatment. J Biomed Mater Res **29,** 1373, 1995.
58. Liu, Y., Chen, F., Liu, W., Cui, L., Shang, Q., Xia, W., Wang, J., Cui, Y., Yang, G., Liu, D., Wu, J., Xu, R., Buonocore, S.D., and Cao, Y. Repairing large porcine full-thickness defects of articular cartilage using autologous chondrocyte-engineered cartilage. Tissue Eng **8,** 709, 2002.
59. Zhou, G., Liu, W., Cui, L., Wang, X., Liu, T., and Cao, Y. Repair of porcine articular osteochondral defects in non-weightbearing areas with autologous bone marrow stromal cells. Tissue Eng **12,** 3209, 2006.
60. Wakitani, S., Goto, T., Pineda, S.J., Young, R.G., Mansour, J.M., Caplan, A.J., and Goldberg, V.M. Mesenchymal cell-based repair of large, full-thickness defects of articular cartilage. J Bone Joint Surg Am **76,** 579, 1994.
61. Hiraide, A., Yokoo, N., Xin, K.Q., Okuda, K., Mizukami, H., Ozawa, K., and Saito, T. Repair of articular cartilage defect by intraarticular administration of basic fibroblast growth factor gene, using adeno-associated virus vector. Hum Gene Ther **16,** 1413, 2005.

Address correspondence to:
Gang Li, M.D., Ph.D.
Stem Cells and Regeneration Research Group
Department of Orthopaedics & Traumatology
Faculty of Medicine
Li Ka Shing Institute of Health Sciences
The Chinese University Hong Kong
Clinical Sciences Building
Prince of Wales Hospital
Shatin, N.T.
Hong Kong, SAR
P.R. China

E-mail: gangli@ort.cuhk.edu.hk

Xiaochun Wei, M.D., Ph.D.
The Orthopaedics Department
The Second Hospital of Shanxi Medical University
Taiyuan 030001
P.R. China

E-mail: weixiaochun06@yahoo.com

Received: July 1, 2009
Accepted: November 4, 2009
Online Publication Date: December 28, 2009